



Circulation adjustment in the Arctic and Atlantic in response to Greenland and Antarctic mass loss

J. van den Berk¹ · S. S. Drijfhout^{1,2} · W. Hazeleger²

Received: 12 November 2020 / Accepted: 29 March 2021 / Published online: 21 July 2021
© The Author(s) 2021

Abstract

Following a high-end projection for mass loss from the Greenland and Antarctic ice-sheets, a freshwater forcing was applied to the ocean surface in the coupled climate model EC-Earthv2.2 to study the response to meltwater release assuming an RCP8.5 emission scenario. The meltwater forcing results in an overall freshening of the Atlantic that is dominated by advective changes, strongly enhancing the freshening due to dilution by Greenland meltwater release. The strongest circulation change occurs in the western North Atlantic subpolar gyre and in the gyre in the Nordic Seas, leaving the North Atlantic subpolar gyre the region where most advective salt export occurs. Associated with counteracting changes in both gyre systems, the response of the Atlantic Meridional Overturning Circulation is rather weak over the 190 years of the experiment; it reduces with only 1 Sv ($= 10^6 \text{ m}^3 \text{s}^{-1}$), compared to changes in the subpolar gyre of 5 Sv. This relative insensitivity of the AMOC to the forcing is attributed to enhanced convection in the Nordic Seas and stronger overflows that compensate reduced convection in the Labrador and Irminger Seas, and lead to higher sea surface temperatures (SSTs) in the former and lower SSTs in the latter region. The weakened subpolar gyre in the west also shifts the North Atlantic Current and the subpolar-subtropical gyre boundary; with the subtropical gyre expanding, and the western subpolar gyre contracting. The SST changes are associated with obduction of Atlantic waters in the Nordic Seas that would otherwise obduct in the western subpolar gyre. The anomalous SSTs also induce a coupled ocean-atmosphere feedback that further strengthens the Nordic Seas circulation and weakens the western subpolar gyre. This occurs because the anomalous SST-gradient enhances the westerlies, especially between 65°N and 70°N; the associated increase in windstress curl consequently enhances the gyre in the Nordic Seas. This feedback is driven by the Greenland mass loss; Antarctic meltwater discharge causes a weaker, opposite response and more particularly affects the South Atlantic salinity budget through northward advection of low-salinity waters from the Southern Ocean. This effect, however, becomes visible only hundred years after the onset of Antarctic mass loss. We conclude that the response to freshwater forcing from both ice caps can lead to a complex response in the Atlantic circulation systems with opposing effects in different subbasins. The relative strength of the response is time-dependent and largely governed by internal feedbacks; the forcing acts mainly as a trigger and is decoupled from the response.

Keywords Meltwater · Atlantic Ocean · Subpolar gyre · Coupled climate models

1 Introduction

✉ J. van den Berk
jellevandenberk@gmail.com; vandenbj@knmi.nl
S. S. Drijfhout
sybren.drijfhout@knmi.nl; s.drijfhout@uu.nl
W. Hazeleger
w.hazeleger@uu.nl

¹ Royal Netherlands Meteorological Institute, De Bilt, The Netherlands

² Utrecht University, Utrecht, The Netherlands

In a warming climate, the increase in atmospheric temperature will also affect the ocean and cryosphere (Pörtner et al. 2019) provides a synthesis of current research on this topic). Apart from heating up the ocean, ice melt—in particular from the Greenland and Antarctic ice sheets—will increase, leading to enhanced freshwater release to the ocean. The direct effect of this meltwater is a decrease in sea surface salinity and a rise in sea level (Bindoff et al. 2007). At low temperatures, the thermal expansion coefficient for sea water is low compared to the haline contraction (Aagaard

and Carmack 1989); for this reason, the impact on density of adding freshwater is largest in a cold environment, e.g. where mass loss from the Greenland and Antarctic ice sheets naturally occurs. A freshwater excess at the northern convection sites (Labrador Sea, Irminger Sea, Nordic Seas) could also have an impact on the ocean circulation by affecting the Atlantic Meridional Overturning Circulation (AMOC) and gyre circulation (Yang et al. 2016).

There is observational evidence that the AMOC has already been in decline since the last decade (Smeed et al. 2018) and this is supported by observed spatial patterns in SSTs (Caesar et al. 2018) that are also seen in climate models. More recent observations (Moat et al. 2020), however, indicate the AMOC is no longer weakening. Additionally, Fu et al. (2020) argue that the current AMOC state is not different from several decades ago and show that within the North Atlantic subpolar gyre (SPG) a stable overturning persists in the eastern part of the basin, as opposed to the Labrador Sea, despite substantial upper-layer water property changes. Since it is unclear whether the observed AMOC weakening in the last decade was due to anthropogenic forcing or part of an internal variation, observations over a longer period are needed. Also, SSTs have changed; the North Atlantic has seen elevated SSTs in the recent several decades of up to 1°C (Bulgin et al. 2020). The spatial pattern of the SST tendencies is not uniform and the largest differences have occurred recently. In particular, there is a cooling south of Greenland ('warming hole') and a stronger increase further south in the Gulf stream region. Mass loss from the polar ice sheets also has become apparent from changes in elevation (Helm et al. 2014). A sixfold increase in Greenland mass loss has been observed since the 1980s (Mouginot et al. 2019), and Antarctic mass loss has also accelerated over the past decades (Paolo et al. 2015).

Ice sheet mass could weaken or destabilise the AMOC and force it into a long-term 'off-state' (e.g. Rahmstorf (1996)). AMOC bistability was first shown to exist in a general circulation global climate model by Manabe and Stouffer (1988). A collapse of the AMOC can have drastic consequences such as cooling of the Northern Hemisphere and warming of the Southern Hemisphere (Vellinga and Wood 2002). Such abrupt changes have also occurred in past AMOC switches and is seen in the Greenland ice core record (Dansgaard et al. 1982; Johnsen et al. 1992). In a study comparing the response in five climate models to a 0.1 Sv (1 Sv = $10^6 \text{ m}^3 \text{ s}^{-1}$) freshwater discharge from Greenland only (Swingedouw et al. 2013); it was found that the AMOC was impacted, but that the weakening depends on the amount of leakage of the freshwater anomaly from the subpolar to the subtropical gyre. In a follow-up study (Swingedouw et al. 2015) it was shown that the AMOC response to the same amount of hosing decreased with global warming in an RCP8.5 scenario (Taylor et al. 2012) run. Increased

stratification due to warming diminished the additional impact of increased stratification due to freshwater discharge in the subpolar gyre. Also, leakage of the additional freshwater to the subtropical gyre increased due to a northward shift of the storm tracks reducing the tilt of the subpolar-subtropical gyre front. In both studies the simulations were only a few decades long and the AMOC response was not yet equilibrated. The impact of freshwater discharge from Greenland on the Nordic Seas can also take place on a longer timescale than its impact on the Labrador and Irminger Seas, because in the former case the freshwater has to recirculate in the subtropical gyre before it reaches the north-east Atlantic, while in the latter case the freshwater already arrives within a few years. The different timescales for Greenland freshwater discharge affecting deep convection sites in the Labrador and Irminger Seas versus the Nordic Seas imply a possibly complex AMOC response to Greenland mass loss, operating at various timescales.

Deep convection in the Labrador, Irminger and Nordic Seas is tightly coupled to the AMOC, as shown by model experiments in which the AMOC weakens when deep convection declines in response to additional freshwater release (Stouffer et al. 2006; Brodeau and Koenigk 2016; Drijfhout 2015). This coupling is corroborated by analysis of the pathways of the lower branch of the AMOC (Lavender et al. 2000; Gary et al. 2011; Rhein et al. 2017) which shows that an interior pathway from the subpolar to the subtropical North Atlantic gyres carries a significant export of deep water. In addition, the AMOC slowdown may trigger a delayed positive feedback by amplifying the freshening over the convection sites through reduced northward transport of salty waters, away from the South Atlantic (Drijfhout et al. 2011; Jackson et al. 2013). On the other hand, after advection of the freshwater anomaly to the eastern side of the subpolar gyre (Swingedouw et al. 2013), the net effect on east-west density (and pressure) gradients of the added freshwater remains small, and this might imply a much weaker impact on zonally averaged northward volume transport than expected from the impact of deep convection alone.

The effect of freshwater discharge from Antarctica might also affect the AMOC and even strengthen it. It has been shown that multi-decadal to centennial timescales in ocean and climate models the AMOC often scales with a north-south pressure (density) gradient (Marotzke 1997; Thorpe et al. 2001; Sijp et al. 2012). This implies that changes in the Southern Ocean can affect the AMOC as well, but on a longer timescale (Weijer et al. 2002; Weber et al. 2007). A more rapid response through wave dynamics is, however, also possible (Swingedouw et al. 2009). A freshwater discharge from Antarctica in that case would act to reduce density and pressure in the south. The effect of Antarctic freshwater release would be to increase the north-south pressure (density) gradient and strengthen the AMOC. For this

reason, it is important to study the AMOC response in a freshwater discharge scenario that accounts for both Northern and Southern Hemisphere sources instead of meltwater discharge from Greenland only (Swingedouw et al. 2013; Weijer et al. 2012; Bakker et al. 2016; Haskins et al. 2020). The calving of icebergs affects spatial patterns of the mass redistribution, especially in the Southern Ocean (Starr et al. 2021).

Here we will investigate the response of the Atlantic circulation to freshwater release from both Northern and Southern Hemisphere sources combined and in isolation, to assess their impact, to what extent these impacts counteract or reinforce each other, and how they change over time. To clearly assess the influence of freshwater discharge from Antarctica in addition to discharge from Greenland, we rely on a scenario where, eventually, mass loss from Antarctica becomes larger (a factor of 2.5) than mass loss from Greenland, in agreement with a scenario in which the West-Antarctic ice sheet starts to collapse (Joughin et al. 2014; Rignot et al. 2014; Feldmann and Levermann 2015; Shepherd et al.

2019) when forced with the RCP8.5 emission scenario. The freshwater forcing scenario includes an iceberg distribution pattern (described in Van den Berk and Drijfhout (2014)) that distributes a freshwater release further away from the ice sheets. This distribution was derived from modelled iceberg drift under current conditions. After 2100 both types of forcing decrease to the initial 2005 values, to emphasise different timescales between forcing and response.

This paper is structured as follows. Section 2 summarises the experimental set-up and presents the framework of the analysis. In Sect. 3 the analysis is shown. A discussion of the main results and final conclusions are presented in Sect. 4.

2 Experiments

The forcing profiles for CO₂ concentration and meltwater release used here are shown in Van den Berk et al. (2019) and reproduced here as Fig. 1. The freshwater release is described in detail in Van den Berk and Drijfhout (2014).

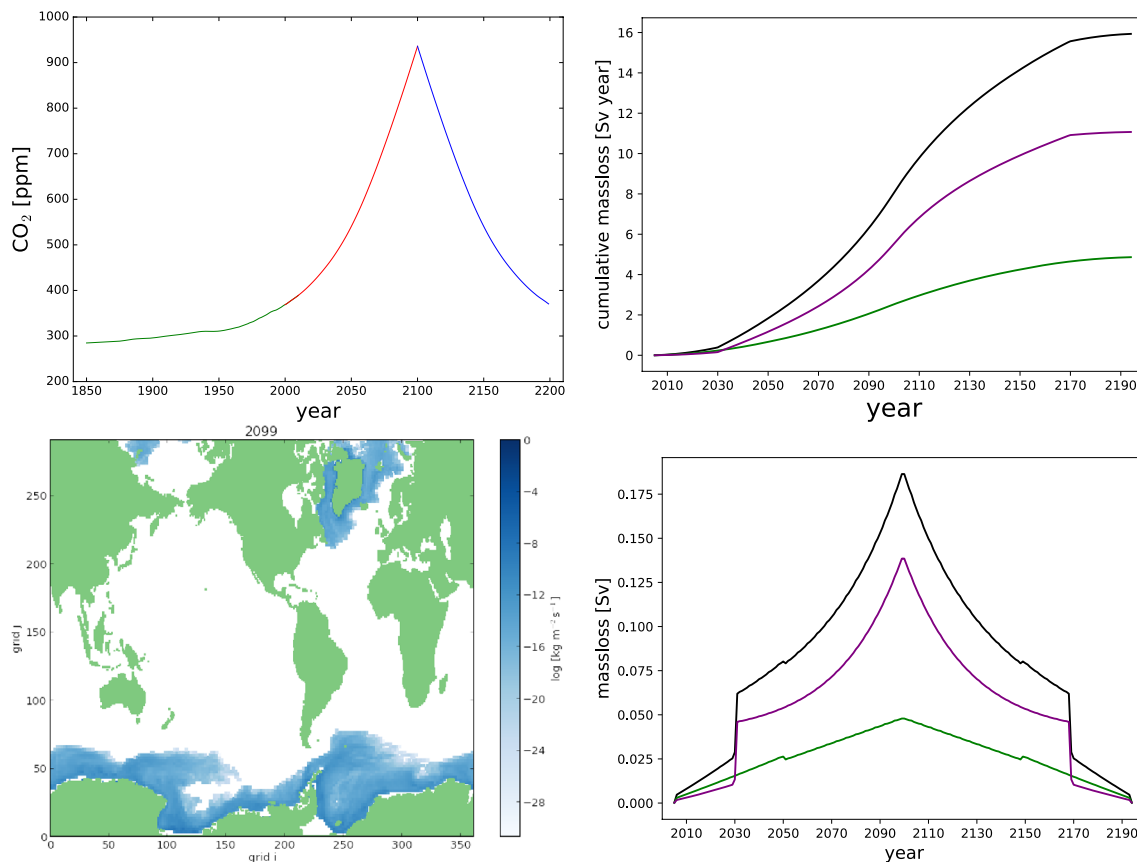


Fig. 1 Top: The two forcing profiles applied in our simulations. Top-left panel: atmospheric CO₂ concentration. In green the historical phase (after which our simulation start), in red the ‘ramp-up’ phase with increasing CO₂, and in blue the ‘ramp-down’ phase as a counterpart to the ramp-up. Top-right panel: cumulative global freshwater

forcing (global: black, northern hemisphere: green, southern hemisphere: purple). Bottom-left: iceberg melt pattern (see Van den Berk and Drijfhout 2014, for technical details). Bottom-right: melt rates; the top-right panel shows the time-integrated curves of these. Reproduced from Van den Berk et al. (2019)

In summary, until year 2100 there is an increase in both forcing timeseries, followed by a time-symmetric decrease of the forcing until year 2195. The freshwater discharge from Greenland increases from 0 Sv in the year 2005 when the RCP scenarios start, to 0.07 Sv in year 2100; after which it decreases again to 0 Sv in 2195; for Antarctica the value in year 2100 is 0.17 Sv. These numbers lead to 71.5 cm sea-level rise in year 2100 due to mass loss from ice sheets only, which is large but not unrealistic. For instance, the value for the 83rd percentile (the upper bound of a likely range of 2/3) in a RCP8.5 scenario given in Bamber et al. (2019) is 102 cm. The two phases (before and after year 2100) are labelled ‘ramp-up’ and ‘ramp-down’ (see also Sgubin et al. (2014) for a similar experimental set-up). The atmospheric forcing follows the RCP8.5 scenario (Taylor et al. 2012) during the ramp-up; the freshwater forcing timeseries is described in more detail in Van den Berk and Drijfhout (2014). The control experiment *C* does not include the meltwater forcing, while *H* includes forcing in both hemispheres. Northern Hemisphere-only freshwater forcing (*N*) and Southern Hemisphere-only freshwater forcing (*S*) each have one single member, *C* and *H* each have four members (see Table 1 for an overview of all runs). All output was saved as monthly mean values.

The experiments are performed with the Coupled Climate Model (CCM) ‘EC-Earth’ which consists of three components. The atmosphere and land surface are modelled with the Integrated Forecast System (IFS–cycle 31r1) which resolves 62 layers in the vertical and uses a triangular truncation at wavenumber 159 (ECMWF 2007) (effectively resolving ≈ 130 km). The ocean is modelled by the Nucleus for European Modelling of the Ocean (NEMO) developed by the NEMO European Consortium at a resolution of approximately 1° in the horizontal (≈ 110 km at mid latitudes) and 42 levels in the vertical (Madec 2008). The two are synchronised along the interface every three model-hours by the OASIS3 coupler developed at the Centre Européen de Recherche et de Formation Avancée en Calcul Scientifique (Valcke et al. 2004). The ocean model is coupled to a sea-ice model developed by the University of Louvain-la-Neuve (LIM2) (Fichefet 1997; Bouillon et al. 2009). The general

characteristics of EC-Earth simulations are described by Hazeleger et al. (2012), Sterl et al. (2012) describes the ocean aspects in greater detail. Sterl et al. (2012) note that the overturning strength shows 2 Sv fluctuations on decadal scales, and these variations are driven by ocean temperature variations. Wouters et al. (2012) note that AMOC fluctuations in EC-Earth are not directly forced by the atmosphere, but are delayed responses to the ocean being forced by the North Atlantic Oscillation (NAO, Hurrell (1995)) on a 60-year timescale.

In response to the freshwater forcing, the salt balance in the ocean is expected to differ by latitude as the freshwater spreads out through the ocean. Apart from the extra freshwater forcing applied, the salinity is affected by ocean advection and changes in evaporation, precipitation, run-off, and changes in sea-ice volume (E-P-R-I). To gain insight into the processes that change the ocean’s salinity we consider regional budgets according to the partitioning shown in Fig. 2 which divides the Arctic+Atlantic basin into four boxes with five zonal sections as boundaries between them and the rest of the ocean. The first box is the Arctic ocean, and box 2 and 3 contain the subpolar and subtropical North Atlantic gyres, respectively; the fourth box is the remainder of the basin (South Atlantic) with the cut-off placed at the section connecting Cape Agulhas with South America. There is one meridional section through the Strait of Gibraltar in box 3.

In the next section, salt advection is decomposed into three components: overturning, azonal (gyre), and barotropic flow. Transport changes are also decomposed in a part driven by changes in volume transport and a part driven by changes

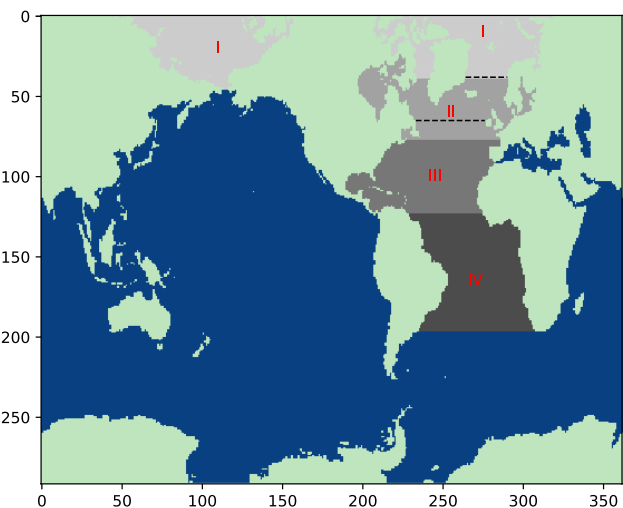


Fig. 2 Basin partitioning on the model grid (ORCA 1). I: Arctic, II: subpolar gyre, III: subtropical gyre, IV: South Atlantic. Boundaries are at 34°S and (9, 47, 67)°N, (67°N is the latitude of Bering Strait). These four areas extended to depth are referred to as boxes 1–4 in the text. Dashed lines indicate sections at 70°N and 55°N

Table 1 Overview of experiments and their included forcing

	CO ₂	NH Melt	SH Melt	Members
C	+	-	-	4
H	+	+	+	4
N	+	+	-	1
S	+	-	+	1

The control experiment *C* does not include the meltwater forcing, but *H* includes forcing in both hemispheres. Northern Hemisphere-only freshwater forcing (*N*) and Southern Hemisphere-only freshwater forcing (*S*) each have a single member, *C* and *H* each have four

in salinity. For more details, and the mathematical formulation of these components, we refer to Van den Berk and Drijfhout (2014) and Van den Berk et al. (2019).

3 The salt redistribution within the Atlantic basin

The freshwater from the forcing field is not uniformly spread throughout the World Ocean as shown in Fig. 3. In the North Atlantic, the shape of the salinity anomaly on the subpolar/subtropical interface suggests that the subpolar gyre redistributes the freshwater from the forcing and that significant exchange with the subtropical gyre occurs (similar as seen in Swingedouw et al. (2013)). Near the Antarctic Peninsula, the Antarctic Circumpolar Current (ACC) distributes the freshwater originating from Antarctica northward in the Southern Ocean. Also, there is a lag of 50 years before salt is exported from the Southern Ocean into the South Atlantic across the Agulhas section (see Van den Berk et al. 2019).

While the basin-integrated freshwater budget is dominated by adjustments at the southern boundary of the South Atlantic (Van den Berk et al. 2019), Fig. 3 shows that the largest changes in freshwater transport occur within the North Atlantic. Freshwater changes induced by anomalous salt advection strongly differ per region, as is shown in the top panel in Fig. 4.

The difference between the simulations with the freshwater forcing and the control runs is a residual signal for barotropic, overturning, and gyres salt transports. As is shown below, the barotropic and overturning transport residuals nearly cancel each other between the subpolar gyre (SPG)

and subtropical gyre (STG), leaving a small net effect that is dominated by adjustment of the gyre in the SPG. Between the SPG and Arctic, however, there is a near cancellation between the gyre components, leaving a residual that is dominated by changes in barotropic and overturning transports.

Below we first focus on the interaction between the Arctic and the North Atlantic subpolar gyres (Sect. 3.1). We proceed with the interaction between the North Atlantic subpolar and subtropical gyres (Sect. 3.2) that gives rise to the peculiar salt redistribution seen in the North Atlantic in Fig. 3. The South Atlantic shows little response and will not be discussed in detail.

3.1 Salt exchange between the Arctic and subpolar North Atlantic

Figure 4 shows a counteracting signal in the gyre-driven salt advection between the Nordic Seas and the North Atlantic subpolar gyre. This change in transport is dominated by velocity changes in the subpolar gyre, as illustrated by Fig. 5. This figure shows plots of the net salt advection for the four boxes decomposed into components associated with salinity (S) and velocity (V) changes. In the subpolar North Atlantic anomalous salt transport by the gyre freshens the North Atlantic by increasing the net export of salt to the Arctic where the gyre salinifies the basin (Fig. 5, dash-dotted lines). To understand this further we investigate the change in vertically-averaged horizontal circulation in the North Atlantic. The subpolar gyre shows a decrease in strength in the west (as seen in the barotropic streamfunction in Fig. 6), while the gyre circulation in the Nordic Seas becomes stronger. The gyre causes more salty water from the North Atlantic

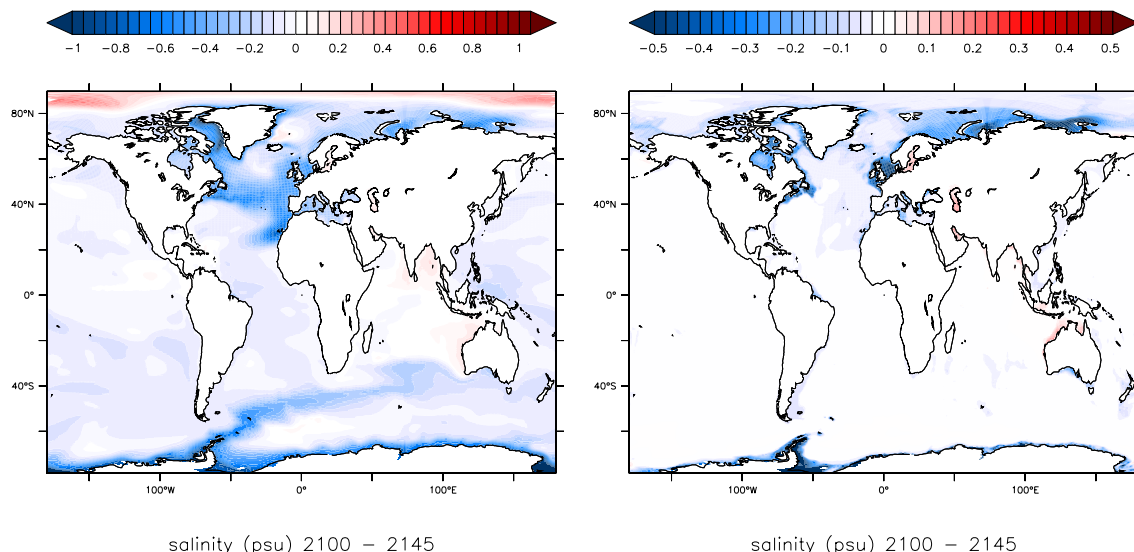
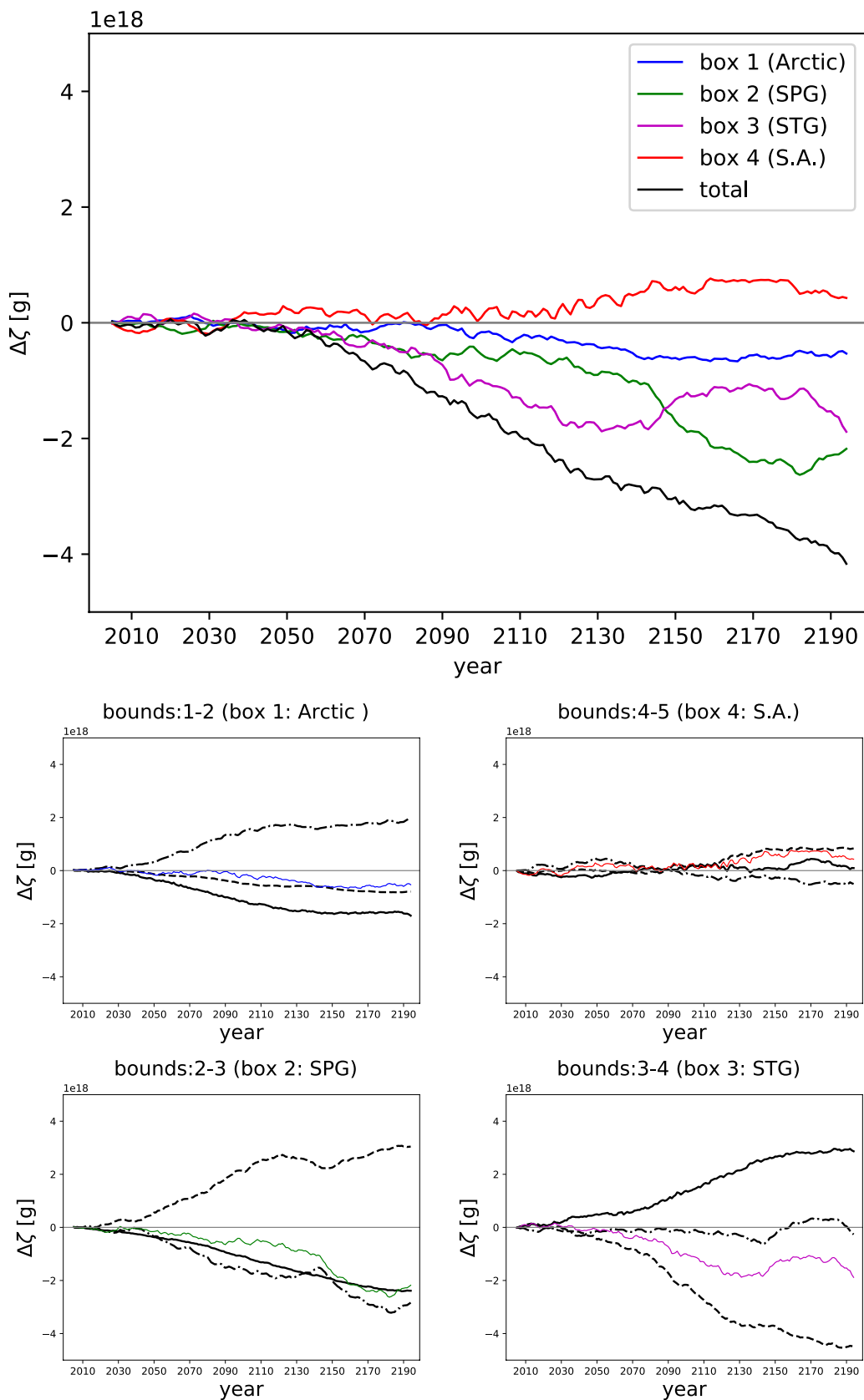


Fig. 3 Left: Ensemble-averaged 45-year averaged surface salinity anomaly ($H - C$) and right: depth-averaged salinity anomaly ($H - C$) after 95–140 years of forcing. Note the difference in scale between the panels



◀Fig. 4 Anomaly ($H - C$) of time-integrated salt advection. Top panel shows the total salt advection anomaly across each box (i.e. depth-integrated north-south differences) and for the Arctic+Atlantic together. The panels below have the salt advection across the indicated box(es) split into three dynamic components: barotropic (solid line), overturning (dashed line), and azonal or gyre (dash-dotted line); sum values correspond to those in the top panel. Ensemble averages

Current to be drawn into Arctic while the return flow in the East Greenland Current becomes fresher, explaining the salinity-driven component in salt-increase in the Arctic by the gyre (Fig. 5, dash-dotted lines in left panels). This raises the question: which processes are responsible for the change in gyre strength? And more specifically, is the change purely an ocean-driven adjustment or does it involve atmospheric feedbacks?

3.1.1 Forcing and transport response

First, we investigate whether changes in buoyancy and wind-stress forcing can account for the change in gyre circulation. Between Scotland and Iceland the North Atlantic Current diverges into two main pathways; one branch feeds the subpolar gyre and another feeds the Nordic Seas by continuing past Iceland. The weakening of the subpolar gyre leads to warmer and saltier water bypassing the subpolar gyre and travelling, via the Norwegian Current, into the Nordic Seas. As a result, within the subpolar gyre SST decreases and heat loss to the atmosphere decreases, leading to a net heat gain by anomalous surface buoyancy fluxes (Fig. 7). This is especially noticeable in the two main convection sites in the Labrador and Irminger Seas where we note a greater increase in downward buoyancy flux (less heat loss to the atmosphere) than in other parts of the subpolar gyre. In the Nordic Seas the opposite occurs, where the buoyancy flux increase is dominated by the thermal forcing (Fig. 7). Note that the changes in the haline component of the buoyancy flux are much smaller and can be neglected in the anomalous response. Changes in sea ice due to the freshwater forcing are also negligible.

The surface buoyancy forcing can modify the potential vorticity of the flow and drive an anomalous gyre circulation (Luyten and Stommel 1986; Colin de Verdière 1989). To estimate the buoyancy-forced change on gyre transport, the buoyancy flux is calculated from the net heat flux Q_H [$\text{J s}^{-1}\text{m}^{-2}$] and net freshwater flux (precipitation–evaporation) $P - E$ [$\text{kg m}^{-2}\text{s}^{-1}$] (Karstensen and Lorbacher 2011) as

$$B = \frac{g}{\rho_0} \left[\alpha \frac{Q_H}{C_H} + \beta(P - E) \frac{S}{1 - S/10^3} \right],$$

with α [K^{-1}] and β [kg g^{-1}] the thermal and haline expansion coefficients, respectively; C_H [$\text{J kg}^{-1}\text{K}^{-1}$] is the heat capacity of sea water (taken as constant) and S [psu] is the salinity.

The units of B are m^2s^{-3} . The values of the expansion coefficients can be determined (at surface pressure $P = 0$) from the TEOS-10 polynomial approximations (Intergovernmental Oceanographic Commission and others 2010). The buoyancy flux induces a vertical velocity at the base of the (upper) mixed-layer in a simple two layer approximation (Luyten and Stommel 1986). By defining a reduced gravity g' between the first layer at depth ML , and the deeper ocean (D) below,

$$g' = g \frac{\rho_D - \rho_{ML}}{\rho_0},$$

we can relate a buoyancy forced interfacial velocity W_b to the buoyancy forcing as

$$W_b = -B/g'.$$

This velocity can then be used with the vertically integrated vorticity equation to estimate the contribution to the gyre's mass transport V_b that is forced by heating or cooling:

$$\beta V_b = f \int_{x_e}^{x_w} W_b \, dx. \quad (1)$$

These buoyancy forced changes in gyre transport occur via SST-changes related to changes in circulation; that is, they act as a feedback on already initiated changes by another process which must be the wind-driven response of the gyre. We can determine the depth-integrated Sverdrup transport V_w from the Sverdrup balance,

$$\rho_0 \beta V_w = \int_{x_e}^{x_m} \frac{\partial \tau_y}{\partial x} - \frac{\partial \tau_x}{\partial y} \, dx, \quad (2)$$

with ρ_0 (= 1020 [kg m^{-3}]) the model reference density, β [$\text{s}^{-1}\text{m}^{-1}$] the meridional variation of the Coriolis-frequency, and τ the windstress vector [N m^{-2}]. We integrate from the East coast (x_e) to the extremum of the barotropic stream function (x_m) to avoid the boundary current in the West, where the Sverdrup balance ceases to hold. With these expressions we can compare the effects of wind and buoyancy forcing on transport changes in the gyre of the Nordic Seas and in the western subpolar gyre.

From Fig. 8 it is apparent that the anomaly of the wind-driven Sverdrup transport (dashed line) in the Nordic Seas only partly explains the changes in the barotropic stream function (left panel; solid line), which increases to 5 Sv in 2190 and yielding a positive trend that is still large in 2190. The change in gyre transport in the Nordic Seas can only be attributed for about 50% to changes in the wind; the other half is forced by changes in surface buoyancy flux. The change in subpolar gyre strength in the west (right panel) is of the opposite sign and in 2190 of the order of 4 Sv and also not equilibrated (still decreasing). It is

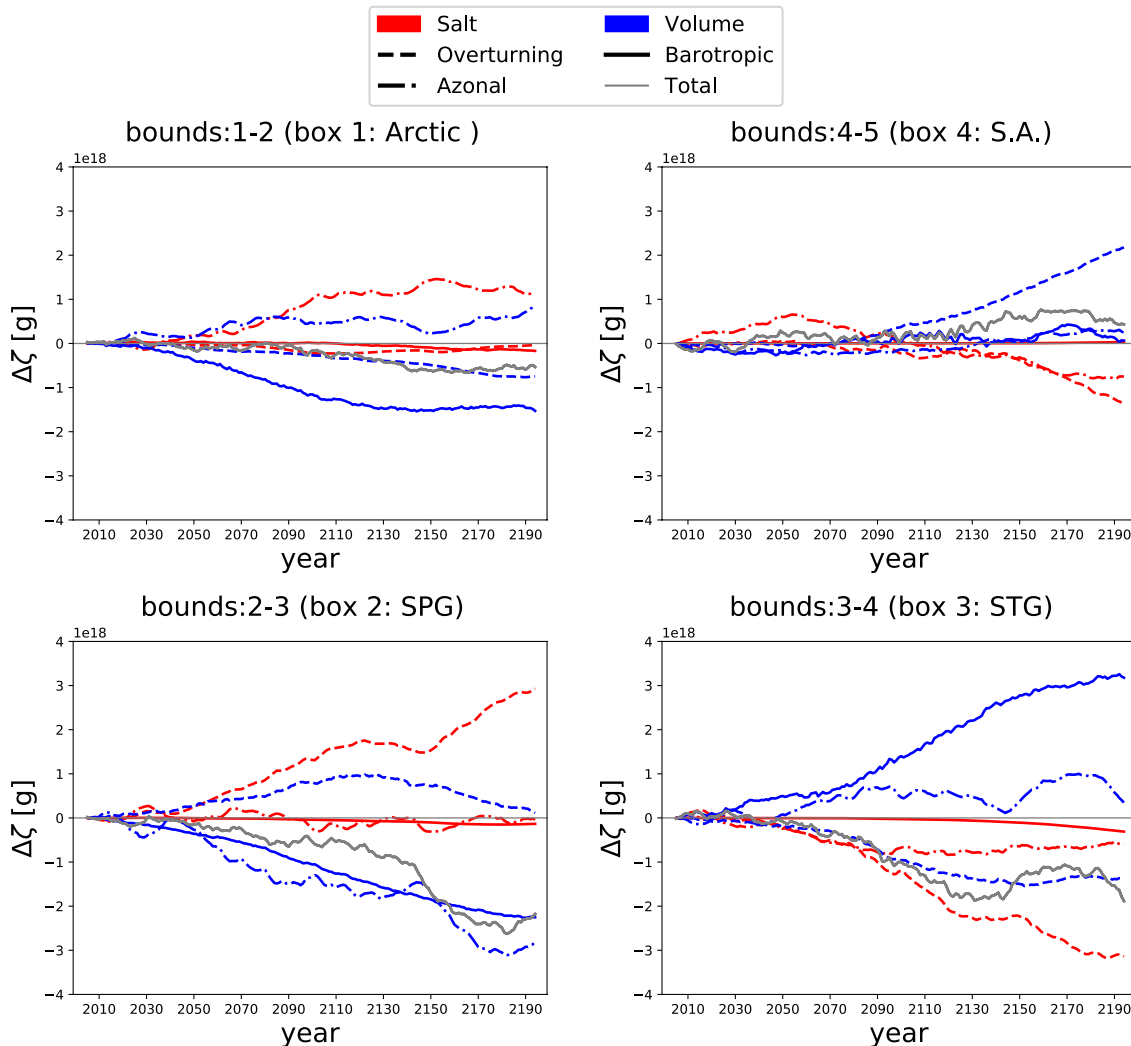


Fig. 5 For indicated boxes, anomaly ($H - C$) of time-integrated salt advection decomposed into a barotropic (solid line), overturning (dashed line), and gyre (dash-dotted line) component, and each

split further into S (salinity driven, red) and V (volume driven, blue) driven parts. Grey lines are their sums (total salt advection through the box). Ensemble averages

Fig. 6 Barotropic streamfunction anomaly ($H - C$), with climatology imposed as contours (solid line as clockwise flow, dashed line as counter clockwise flow, horizontal lines indicate the separation of the STG/SPG), mean of years 2005–2195, ensemble average

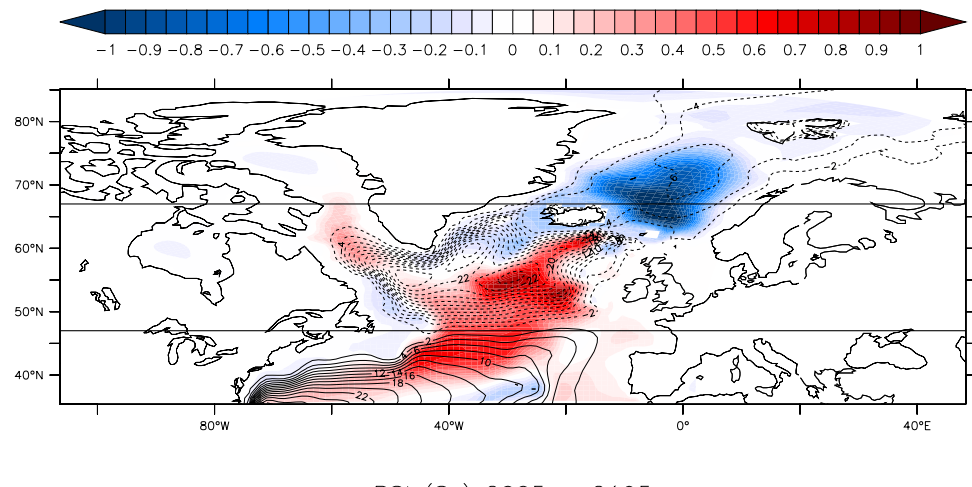
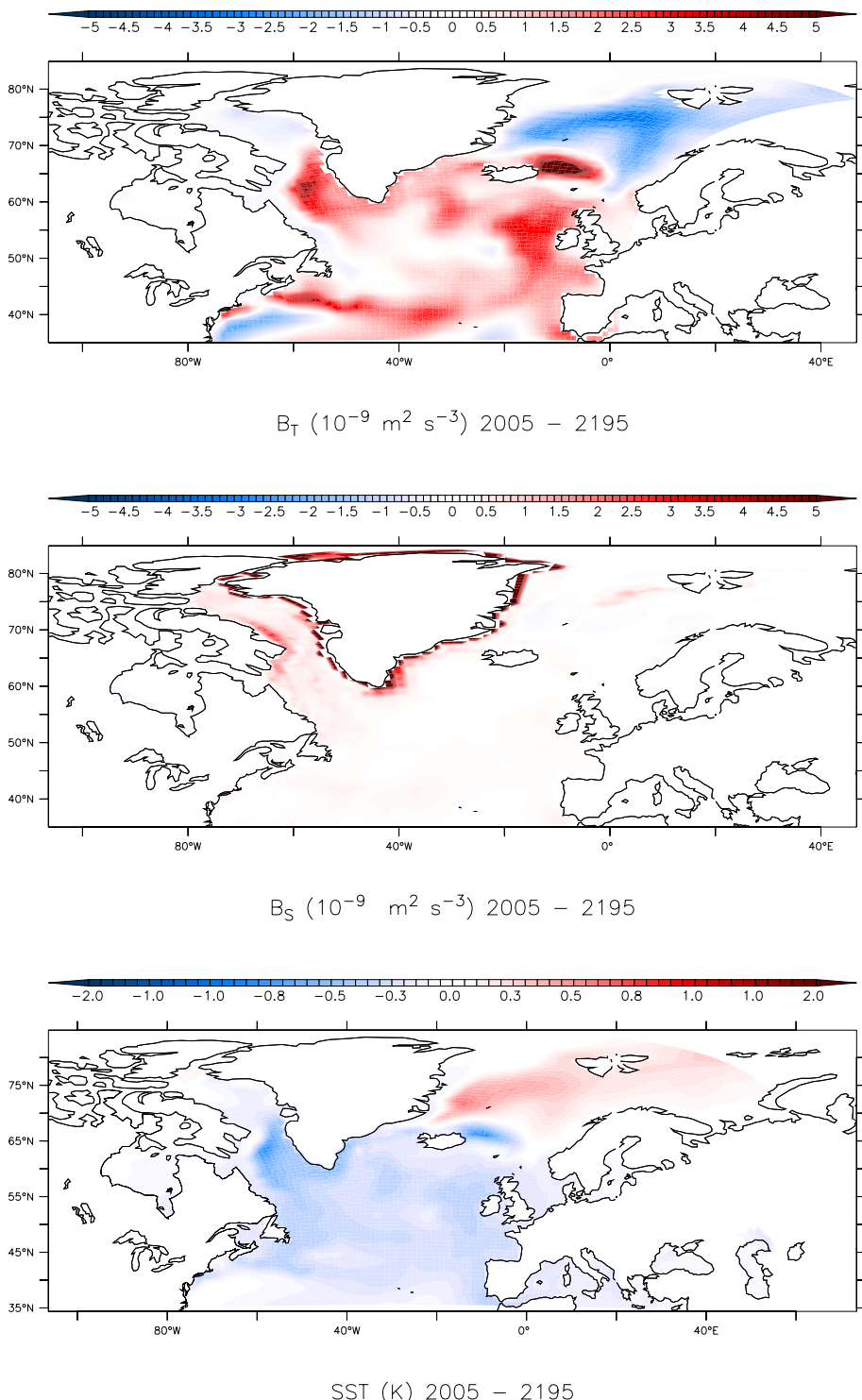


Fig. 7 Mean thermal-buoyancy flux anomaly (top), haline-buoyancy flux anomaly (middle) and SST anomaly (bottom). The SST decreases in the SPG, leading to a decrease of heat flux into the ocean, which results in a lack of buoyancy loss in the SPG. The Nordic Seas show the opposite pattern. Mean of years 2005–2195, ensemble averages ($H - C$)



almost completely forced by buoyancy forcing changes. In both cases the largest changes occur after 2100 when the forcing is decreasing, highlighting the decoupling between forcing and response and the role of internal feedbacks in the coupled climate system. In Fig. 8 we have used mixed-layer depths of 100 m and 200 m to determine the sensitivity of the estimated interfacial velocity due to surface

buoyancy fluxes to the depth of this layer. It appears that at 70°N a mixed-layer depth of 100 m gives a better fit, while at 55°N a mixed-layer depth of 200 m does. It should be stressed that the gyre response to changes in buoyancy (and wind) forcing cannot be fully explained by the forcing at one particular latitude. The velocity changes are more complex than can be captured by a simple two-layer model

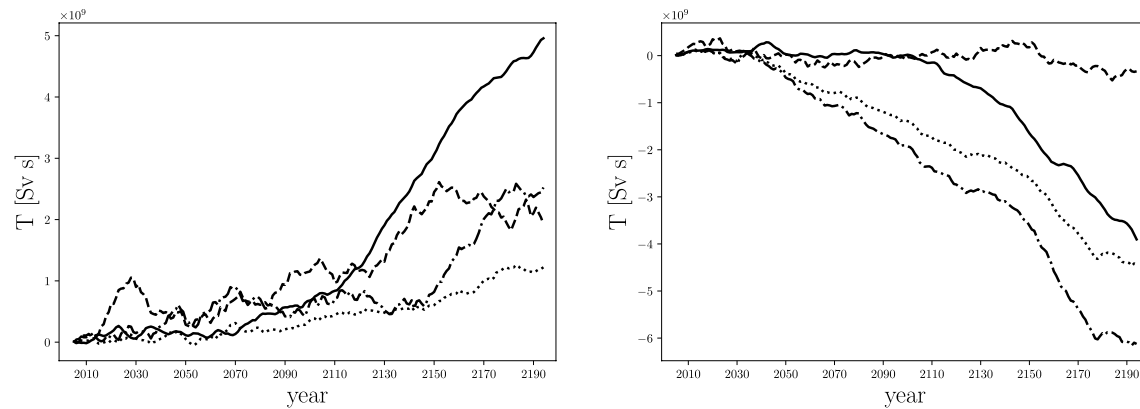


Fig. 8 Time-integrated Sverdrup transport anomaly (V , section-integrated windstress curl scaled with $\rho_0\beta$) (dashed line), time-integrated anomaly of the (extremum of the) barotropic streamfunction (excluding the western boundary current, solid line), and meridional transport due to buoyancy-forcing changes (dash-dotted: 100 m,

dotted: 200 m mixed-layer depth, Eq. 1). Left panel: (70°N) East of Greenland to Norway. Right panel: 55°N (from Ireland to 25°W to avoid the recirculation cell in the SPG to the west of that longitude). Ensemble averages ($H - C$)

and we cannot expect to fully close the volume transport changes per section with this (crude) method. A more detailed analysis such as done in Le Corre et al. (2020) might give further insight.

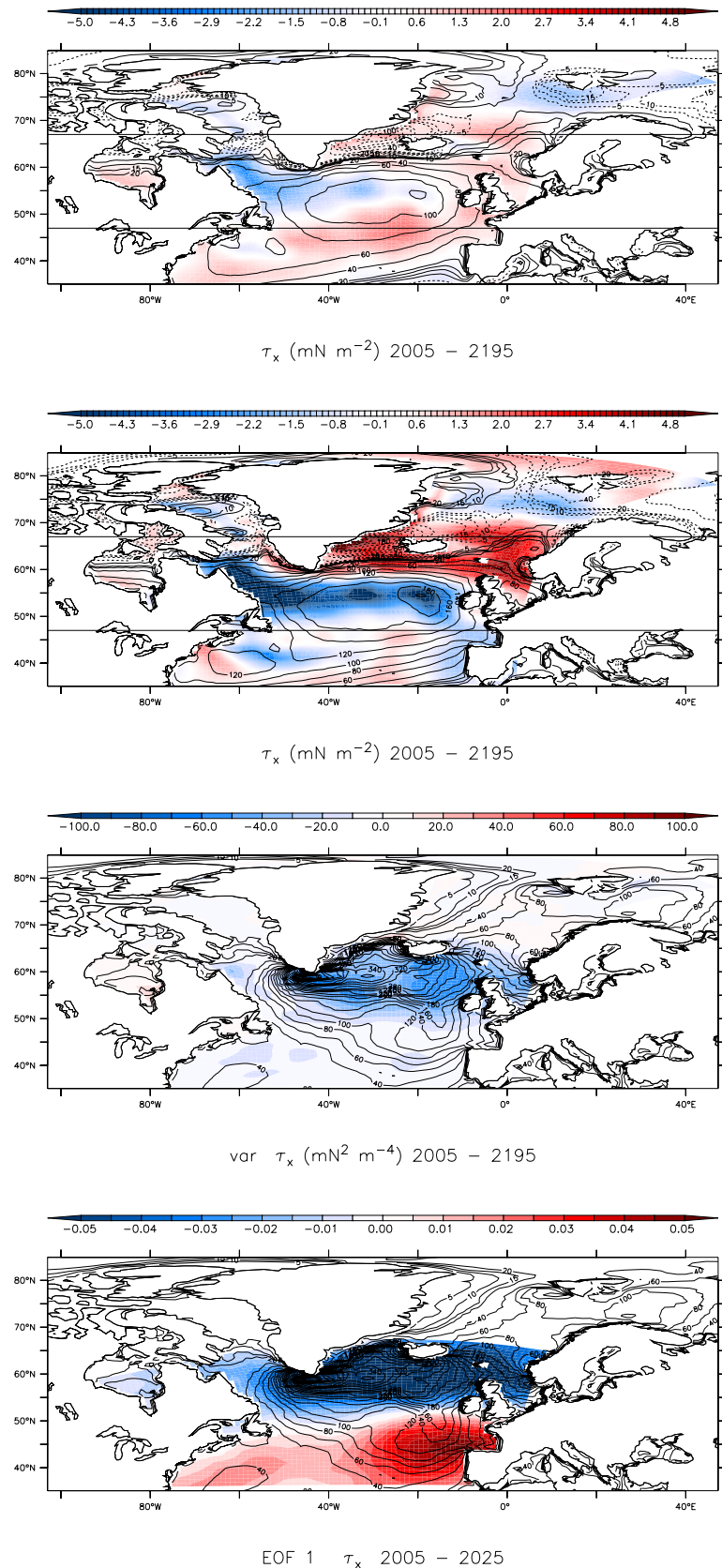
The (winter) wind-response in the Nordic Seas gyre is likely initiated by changes in SSTs and air-sea heat fluxes and thus consists of a coupled ocean-atmosphere feedback, which can be explained by the different SST responses between subpolar gyre in the west and the gyre in the Nordic Seas (Fig. 9). The long-term change in wind stress over the North Atlantic in response to freshwater forcing from Greenland during a strong greenhouse emission scenario ($H - C$) shows increased westerlies at the latitude of Iceland and decreasing westerlies to the south of it centred around 55°N, with again an increase centred around 45°N. This corresponds to a southward shift of the westerly jet stream, but an enhancement of its northerly extension over the British Isles and Scandinavia (i.e. a reduced zonal extent) and a decrease of easterlies between Greenland and Iceland (Fig. 9a). This shift is dominated by the response in winter (Fig. 9b), with the exception of the increase in westerlies around 45°N which is dominated by spring and autumn (not shown). Over the length of the simulations the variance (dominated by the winter months) in the hosing ensemble (H) strongly decreases over the North Atlantic subpolar gyre (Fig. 9c). The pattern of change in interannual variance corresponds well with the NAO pattern, which has a similar pattern in all simulations (Fig. 9d shows the NAO in the control run C). The northern pole of the NAO-dipole overlaps with the spatial distribution of change in variance. Apparently the changes in variability are primarily due to the pattern of dominant North Atlantic atmospheric variability, the NAO, which has also been associated with the storm track variability (Hurrell 1995; Hurrell et al. 2003).

Warming of the Nordic Seas peaks around 70°N; south of 67°N cooling prevails, and is associated with a weaker and fresher subpolar gyre. As a result, a positive northward SST-gradient anomaly weakens the overall north-south-temperature gradient, which reduces westerly winds south of 70°N, while north of 70°N the SST-gradient anomaly enhances the westerlies. This differential wind response then enhances the windstress-curl, and subsequently the Ekman pumping and northward Sverdrup transport across 70°N (Pedlosky 1996).

In Fig. 10 similar transports are seen as in Fig. 8, but for ($N - C$), indicating that the Greenland meltwater forcing is the dominant driver in the Nordic Seas-SPG seesaw effect. Also, in observations an effect of the subpolar gyre and Nordic Seas has already been suggested (Dukhovskoy et al. 2019), although it was argued that it could not be explained by Greenland meltwater discharge alone and the propagation of salinity anomalies from lower latitudes could also play a role. The increase in the wind-driven transport anomaly seen in Fig. 8 is absent, but the observed change in volume transport is less well explained by the two-layer model for the runs with only 1 ensemble member. It could also be that the wind-response, at least partly, must be attributed to the arrival of the Antarctic freshwater anomaly impacting the North Atlantic gyres. This is supported by the fact that in ($S - C$) the changes in volume transport in the northern North Atlantic and Nordic Seas oppose those seen in ($H - C$), especially after year 2100 (not shown).

When the subpolar gyre weakens, isopycnal doming in the middle and the preconditioning for deep-convection reduce, limiting the depth of the winter mixed-layer. This response is thus consistent with reduced convection, while the response in the Nordic Seas gyre is consistent with increased deep convection. Freshening of the subpolar gyre can therefore push the system to a weaker circulation

Fig. 9 Top (a): mean value of the zonal windstress 2005–2195 for the winter months (December, January, February); annual mean climatology imposed as contours. Horizontal lines indicate the zonal sections of the SPG box (2). Middle-top (b): as above, but for the winter months (December, January, February) only. Middle-bottom (c): mean variance 2005–2195. Ensemble average ($H - C$); contours are annual mean values of 2005–2025. Bottom (d): First principle component (EOF) of 2005–2025 capturing 47% of the variance



EOF 1 τ_x 2005 – 2025

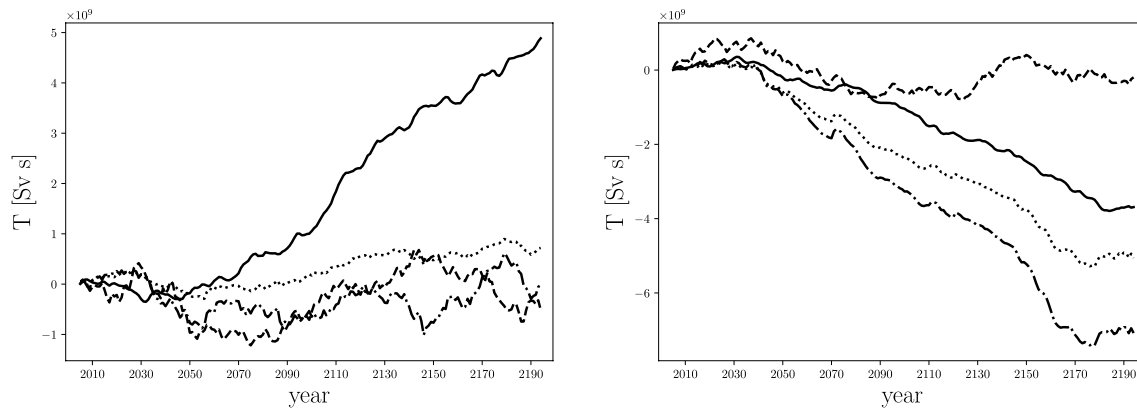


Fig. 10 Time-integrated Sverdrup transport anomaly (V , section-integrated windstress curl scaled with $\rho_0\beta$) (dashed line), time-integrated anomaly of the (extremum of the) barotropic streamfunction (excluding the western boundary current, solid line), and meridional transport due to buoyancy-forcing changes (dash-dotted: 100 m, dotted:

200 m mixed-layer depth, Eq. 1). Left panel: (70°N) East of Greenland to Norway. Right panel: 55°N (from Ireland to 25°W to avoid the recirculation cell in the SPG to the west of that longitude. Ensemble averages ($N - C$)

mode. The mechanism for gyre adjustment discussed here resembles the one found in conceptual and coupled climate models where it was demonstrated that the subpolar gyre may switch from a strong to a weaker mode due to feedback mechanisms involving the stratification in the gyre (Born and Stocker 2013). Here, also coupled feedbacks through an atmospheric response are instrumental in the observed gyre changes. The opposite, however, might also occur: the decrease of convection could weaken the gyre, which in turn affects the salinity in the gyre centre. Because the salinity affects the convection, a positive feedback loop would be present (Born et al. 2016).

3.2 Changes in AMOC salt transport between subpolar and subtropical latitudes

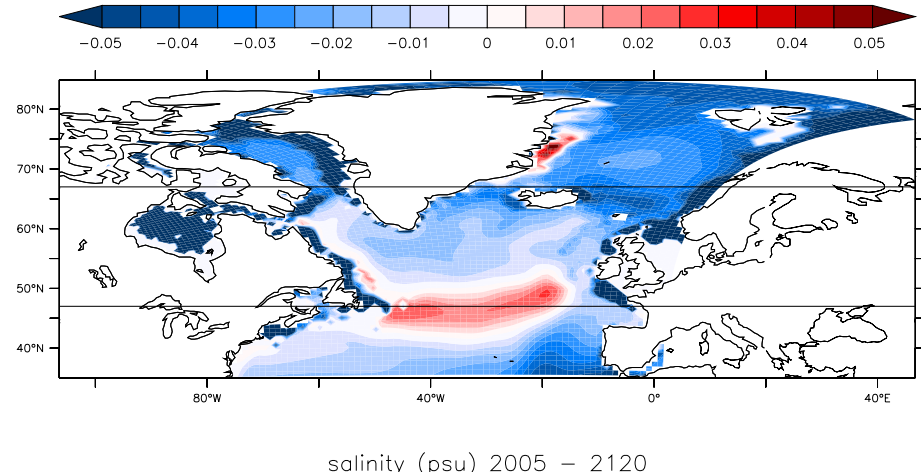
The anomalies of the overturning salt-transport make the subpolar gyre saltier and the subtropical gyre fresher. The

change in salinity is the main reason, not volume change (AMOC strength) (Fig. 5, red dashed versus blue dashed lines).

Enhanced northward salt transport by the overturning across the subtropical/subpolar gyre boundary in response to freshwater release from Greenland is surprising, as in general the surface waters contain larger freshwater anomalies than the deeper waters (compare the left and right panel in Fig 3). This suggests that below the surface more salt is transported northward.

In Fig. 11 it can be seen that a subsurface increase in salinity along the section between the two gyres is the cause for the enhanced northward salt transport by the overturning circulation. The surface has become fresher due to the freshwater release, but the first 1000 m below the surface have become saltier. Comparing with Fig. 6, we see that the subtropical gyre increases (spin-up) and expands while the subpolar gyre weakens and contracts (spin-down). As

Fig. 11 Averaged salinity anomaly ($H - C$) over 100 m–1000 m depth, mean of years 2005–2120. Horizontal lines indicate the zonal sections of the SPG box (2). Ensemble average



a result, the inter-gyre boundary shifts to the North, leaving a positive salinity anomaly along the section chosen to coincide with the gyre boundary in the control run as seen in Fig. 11. The shift in gyre boundary, which is also the boundary between high and low salinity waters, is associated with a small latitudinal band in which the northward salt transport by the overturning circulation increases.

The overturning circulation also further salinifies the subpolar gyre and freshens the subtropical gyre through changes in velocity (Fig. 5, blue dashed lines). At first sight this is surprising because the AMOC transports salt from the STG to the SPG, a weakening of the AMOC in response to freshwater hosing is expected to result in subpolar freshening and subtropical salinification. The change in AMOC, however, is more subtle.

3.2.1 The change in the AMOC

Over most of the Atlantic, the AMOC initially does not weaken in response to the forcing but slightly increases in strength. This is illustrated by Fig. 12 showing a mild

increase ($\sim 0.5 \text{ Sv}$) at most latitudes during the first 50 years, after which the AMOC starts decreasing.

In Fig. 13 the mean mixed layer depth anomaly ($H - C$) for 2005–2195 is plotted, together with the mean value for 2005–2100 under RCP8.5 (ensemble C). The mixed layer becomes shallower mainly in the Labrador Sea and Nordic Seas in the control simulations. The additional freshwater forcing widens the deep water formation region in the Labrador Sea and shifts it in the Nordic Seas. Also, there is not a significant change in AABW production under the freshwater forcing judged from the mixed layer depth changes in the Southern Ocean (not shown). Consistent with a lack of response in the Southern Ocean, we do not find a bipolar seesaw effect, unlike results from other model studies (e.g. Swingedouw et al. (2009)). The AMOC decreases in the control run (C) and the freshwater forcing weakens it further, inhibiting the recovery (and overshoot) seen in the ramp-down phase.

The initial increase in AMOC strength cannot be understood by how the freshwater along the northern boundary of the Atlantic affects the density (i.e. the freshening seen

Fig. 12 Left top panel: climatology of the Atlantic overturning. Right top panel: AMOC index maximum, solid line at all Atlantic latitudes, dashed line at RAPID location 26.5°N (horizontal lines indicate initial and final values). Bottom panel: time-latitude diagram of the anomaly of the AMOC maximum; maxima are taken below 500 m depth for ensemble averages of $H - C$

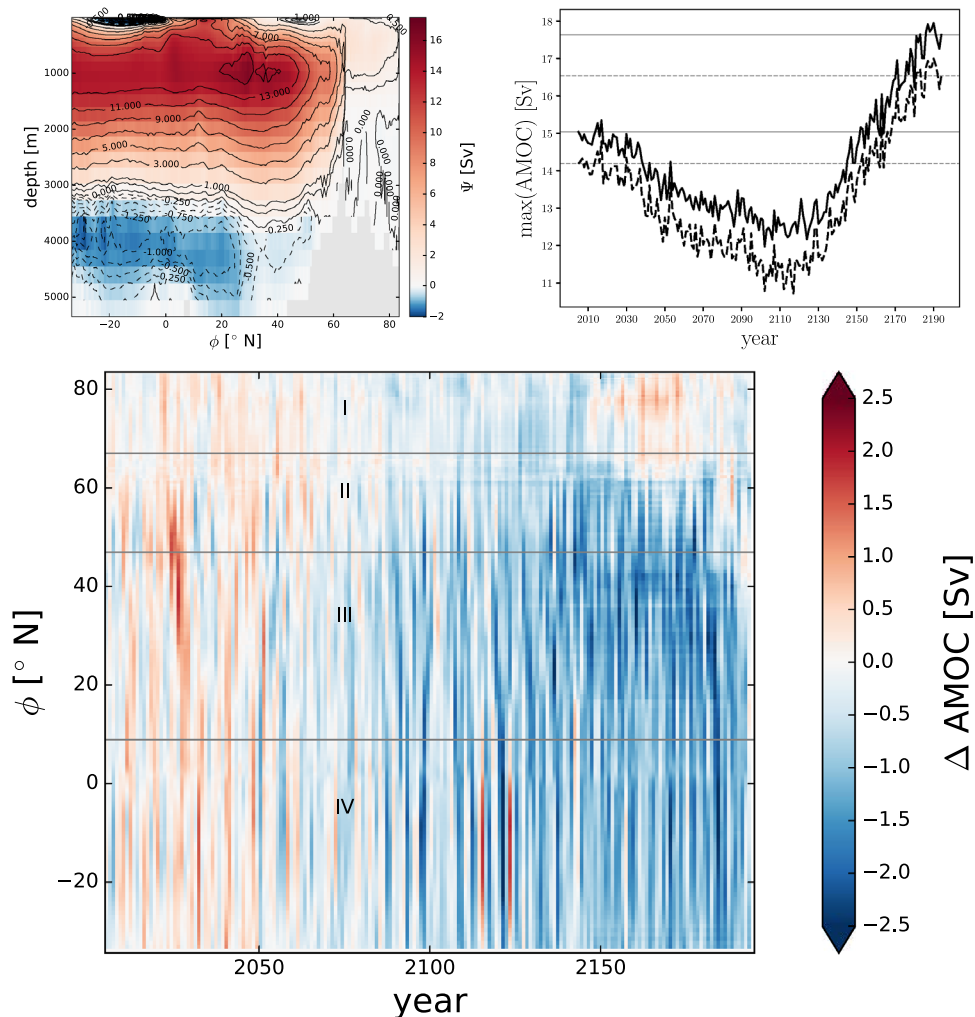
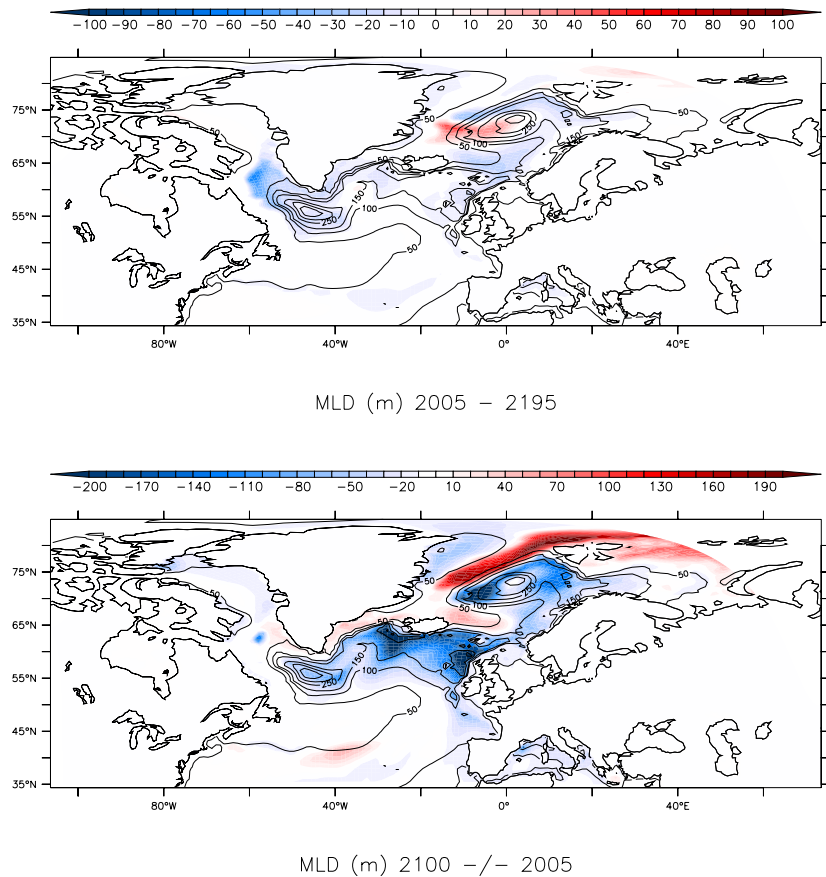


Fig. 13 Top (a): Mean mixed layer depth anomaly ($H - C$) for 2005–2195. Bottom (b): reference annual mean anomaly between 2100 and 2005 under RCP8.5 (C). Ensemble averages. Contours indicate annual mean climatological values



in Fig. 3). To first order, net sinking and AMOC strength scale with the east-west density gradient along the northern boundary of the SPG (Spall and Pickart 2001). The added freshwater induces a negative density anomaly that first affects the western side of the boundary. As a result, the east-west density gradient should increase (which is also seen in Fig. 14), while the AMOC decreases. The argument of Spall and Pickart (2001), however, assumes a direct link between pressure and density gradients, which is only correct under steady-state. Here, a transient source of freshwater is used as a forcing, directly impacting sea surface height (SSH). As a result, the transient freshwater-signal in SSH (volume change) affects east-west pressure gradients as well as the freshening of the water column, and may compensate density changes in a different way as the SSH response to freshening when there is no net volume change in the ocean. Apart from freshening at the western side associated with meltwater release from Greenland, the North Atlantic density fields is also affected by a change in the North Atlantic Current advecting more warm water along the eastern boundary, with less warm water entering the western subpolar gyre, associated with the spin-up of the gyre in the Nordic Seas and a slow-down of the gyre in the western SPG. The surface SSH gradient between the east and west initially overcompensates the decrease in upper

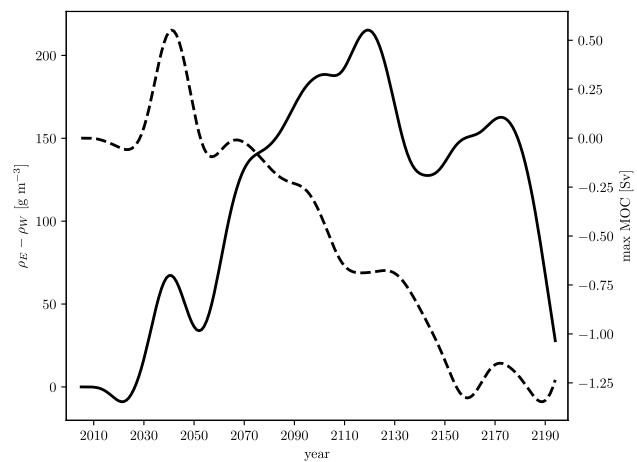


Fig. 14 Solid line is the average potential density anomaly of the East-West difference at the Atlantic section at 60°N of the first 1000 m. The middle 60% of the basin is removed, leaving an eastern and a western side as boundaries. The dashed line is the maximum AMOC over all Atlantic latitudes as shown in Fig. 12. Both lines are shown with a 30-year smoothing (Butterworth filtering) of the time-series applied; ensemble averages ($H - C$)

1000 m density gradient in the sense that it rises faster in the east than in the west, while upper 1000 m density declines faster in the west than in the east (see also Fig. 9 in Van den

Berk et al. (2019) for the spread of the SSH signal). In short, the surface SSH signal spreads faster than the subsurface density anomaly. Fig. 3 shows that the subpolar gyre advects the freshwater anomaly, as it arrives from the Greenland coast, back to the eastern part of the subpolar gyre, between England and Iceland. As a result, the freshwater anomaly affects both the West and the East, leaving a small imprint on the net sinking and there is even a small initial increase in the AMOC (Fig. 14). Only after the year 2050, when the halocline in the Labrador and Irminger Sea becomes strong enough to reduce deep convection there, does the density in the western part of the basin become more strongly affected than in the eastern part and the AMOC starts to decline, now in anti-correlation with the density difference between eastern and western boundary (Fig. 14). This time delay in AMOC-decline is comparable with the circulation timescale of the gyre (Born and Mignot 2012). Note that the decline in AMOC is smaller than in Swingedouw et al. (2013), which is consistent with the smaller Greenland meltwater discharge amount used in this study.

The weak AMOC response to hosing is thus explained by a small change in east-west density and pressure gradients in the North Atlantic due to a switch in convection location. While the freshwater release affects Labrador and Irminger Sea convection, re-stratifying and weakening the western subpolar gyre, this is compensated by enhanced deep convection in the Nordic Seas. Fig. 12 indeed shows an increase of the overturning during the first half of the ramp-up, especially in the Nordic Seas, followed by a small decrease in overturning. The overturning increase in the eastern North Atlantic is indeed coupled to an increased gyre circulation in the Nordic Seas, with a decrease in the western subpolar gyre (Fig. 6), which is consistent with the results described in Zhang et al. (2011).

3.2.2 Changes in AMOC salt transport further south

Both a decreasing AMOC and a decrease in salinity of the upper limb relative to the lower limb contribute to the freshening of the subpolar and subtropical North Atlantic; but remarkably, the salinity driven component of the net salt export by the overturning changes sign after year 2100: up to year 2100 it was importing less freshwater, albeit weakly. This switch is mainly due to changes at the southern boundary of the subtropical gyre (Box 3, Fig. 5) related to freshening of the upper 1000 m of the South Atlantic due to the arrival of meltwater discharge from Antarctica after year 2100. In EC-Earth, the AMOC imports freshwater across the southern boundary of the South Atlantic, a well-known model bias (Mecking et al. 2017). While the weakening AMOC imports less freshwater across the southern boundary of the South Atlantic (Fig. 5), the water that is imported is getting fresher, especially after year 2100. As a result,

the overturning circulation salinifies the South Atlantic by weakening and exporting less salt to the north, but freshens the South Atlantic by importing fresher waters from the Southern Ocean (Box 4, Fig. 5 blue and red dashed lines). The decrease in salt import in the South Atlantic, together with a weaker AMOC, leaves a positive salinity imprint on the North Brazil Current with large-scale freshening further south (Fig. 3 in Van den Berk et al. (2019)). Freshening in the North Atlantic results in freshening of the whole Atlantic, despite the South Atlantic counteracting North Atlantic freshening with an increase in salinity (red line in top panel of Fig. 4), which is however smaller than the freshening in the North Atlantic. However, integrated over the whole basin, this partial compensation is insufficient to counteract the overall freshening (black line in top panel of Fig. 4) and the anomalous transport by the overturning circulation (dashed lines in lower panels of Fig. 4) acts to freshen the Atlantic-Arctic basin through increased freshening of the waters that cross the Agulhas section at 34°S (note that a large fraction of the black line in the top panel of Fig. 4 can be explained by the dashed black in the bottom panels being passed relatively unaffected through the South Atlantic as seen in the right middle panel).

4 Summary and discussion

We investigated the effects of a high-end future climate projection for mass loss from the Greenland and Antarctic ice-sheets. While in response to meltwater discharge the whole Atlantic freshens, freshening occurs unevenly over the sub-basins, with largest freshening in the North Atlantic and even larger, almost compensating adjustments taking place between subpolar and subtropical gyres, while there is little change in the South Atlantic. The two gyres in the subpolar North Atlantic and Nordic Seas respond most strongly. A spin-up of the gyre in the Nordic Seas occurs, in conjunction with a weakening and re-stratification of the subpolar gyre in the west, after the freshwater release decreases Labrador and Irminger Seas convection. A similar seesaw-or shift-between eastern and western convection sites has been described by e.g., Wood et al. (1999), Swingedouw et al. (2013). It causes a weak AMOC response to a Labrador and Irminger Sea convection decrease. As a result, the net deep water formation in the model used (EC-Earth) is not particularly sensitive to Greenland meltwater forcing. A reason for this is the effective re-routing of freshwater by the subpolar gyre away from the convection regions in the West, keeping the decrease in convection there limited. The advective pathways of meltwater release from Greenland, however, may depend on the horizontal resolution of the model and eddy-resolving models might show more freshwater transport from the boundary currents to the sites of deep convection,

especially in the Labrador and Irminger Sea (Lohmann et al. 2014; Yang et al. 2016). Higher resolution is also important for resolving the boundary currents around Greenland, as these determine where Greenland's meltwater is transported to (Gillard et al. 2016). Thus, the AMOC response to meltwater release is determined by how important Labrador and Irminger Sea convection are, relative to convection in the Nordic Seas, and how effective the seesaw between eastern and western convection sites operates (Lozier et al. (2019) discusses the importance of Labrador Sea convection for the AMOC). To what extent the response shown here is model-dependent is unknown and should be investigated by further studies using different climate models with different horizontal resolution.

We should also note some limitations regarding the use of a freshwater forcing field. The meltwater scenarios implicitly account for feedback effects to the freshwater release, but not explicitly the effects on the atmosphere or the secondary effects on the ocean. Interactions with the solid Earth such as isostatic adjustment are already excluded by the model formulation because of the longer timescales involved. The thermal effects are not modelled with a prescribed freshwater forcing. In particular, as the ice sheet melts, more freshwater reaches the oceans and increases stratification, which shallows the halocline. Consequently, more heat is retained near the ocean surface and would increase the basal melt rate. This is a deficiency of only using a freshwater forcing. Another important feedback lacking without a dynamic ice sheet is the interaction with the atmosphere. The geometry of the ice sheet does not change and therefore cannot affect the melt-elevation feedback where a decrease in height of the ice sheet leads to even greater melt due to the warmer temperature at the lower surface after melt. An overview of these feedbacks and others is given in Fyke et al. (2018). Coupling a dynamic ice sheet model to EC-Earth would model some of these feedbacks, but the realism of the resulting effects is not clear.

The effectiveness of the seesaw depends on the feedbacks associated with the gyre spin-up in the Nordic Seas and gyre spin-down in the western subpolar gyre. For instance, Swingedouw et al. (2013) attribute this seesaw between subpolar gyre and Nordic Seas to the increased import of warm and salty Atlantic waters in the Nordic Seas as a result of pathway changes in the North Atlantic Current when obduction in the subpolar gyre no longer occurs. The weakened subpolar gyre leads to a shift in the North Atlantic Current and subpolar-subtropical gyre boundary, with the subtropical gyre expanding and the subpolar gyre contracting. Associated with this shift, deep convection decreases in the subpolar gyre and increases in the Nordic Seas, leading to lower SSTs in the West (less heat transported from the deep ocean to the surface) and higher SSTs in the Nordic Seas associated with increased vertical heat transport to the surface.

In our simulations this change in SSTs induces a coupled ocean-atmosphere feedback that further spins-up the Nordic Seas gyre and spins-down the subpolar gyre. The anomalous SST-gradient associated with this response enhances the westerlies, especially between 65°N and 70°N, and the associated increase in windstress curl further enhances the spin-up of the Nordic Seas gyre. In addition, the anomalous SSTs also affect air-sea fluxes, and the resulting buoyancy forcing acts to further enhance the gyre in the Nordic Seas and to weaken the subpolar gyre in the west. An analysis based on paleo proxies indicates that this seesaw may have played an important role in, especially, the cold phases of Dansgaard-Oeschger oscillations (Wary et al. 2017). A comparison of CMIP5 models (Deshayes et al. 2014), however, shows inconsistent circulation patterns of the subpolar gyre, indicating results are model-dependent. This is another reason more studies—using a variety of models—are needed to assess which response is robust and can be validated by observations. Additionally, it should be noted that the climate model used (EC-Earth) has a bias in the South Atlantic which results in an incorrect sign of M_{ov} (Rahmstorf 1996; Sgubin et al. 2014) (positive, whereas measurements indicate a negative sign Garzoli et al. (2013-01)). A different value for M_{ov} would affect our analysis and the response to the freshwater forcing might be stronger than seen here, especially before 2100.

Observations already suggest subpolar gyre freshening associated with Greenland meltwater discharge and subsequent decrease in Labrador Sea Water thickness (Yang et al. 2016), though natural variability and other freshwater sources from the Arctic play a role as well in the subpolar gyre freshening. In Böning et al. (2016) it was argued that Greenland meltwater discharge may have affected deep convection in the Labrador Sea since year 2010. Claims of earlier signs of Greenland meltwater discharge affecting the AMOC are difficult to sustain, given the signal-to-noise level of this freshwater source against natural variability. The authors also argue that the spreading of the meltwater discharge is intimately linked to mesoscale transport processes, implying that a low-resolution model as used here may not well represent the correct spreading pathways of the meltwater discharge. Another issue is the vertical mixing of the freshwater anomaly. In Dukhovskoy et al. (2019) it is argued that in a regional high-resolution model the mixing is too large for the meltwater discharge to explain the observed signal.

Although we do not see a clear mode switch in the subpolar gyre from a strong to a weak state it appears that similar feedbacks involved in the bi-stability of the subpolar gyre as described in Born and Stocker (2013) do act to weaken the gyre here. The interior pathways of the most northerly AMOC flows are due to buoyancy loss in the Nordic Seas and an increased inflow in the Nordic Seas

can reduce the subpolar gyre further south (Zhang et al. 2011). This is also seen in Sgubin et al. (2017), where CMIP5 models were analysed for abrupt convection collapse events in the Labrador Sea; models showing such a collapse under future anthropogenic emission scenarios most often feature a surprisingly weak AMOC response due to a coincident enhancement of deep convection in the Nordic Seas. The seesaw pattern between the subpolar North Atlantic and Nordic Seas may also explain the remarkable insensitivity of the AMOC to Greenland meltwater discharge. Compared with hosing experiments in which the whole AMOC collapses (Stouffer et al. 2006; Drijfhout 2015), our experiments seem to require larger volumes of freshwater to inhibit both Labrador/Irminger Sea deep convection and deep convection in the Nordic Seas. It appears that the freshwater does not reach the Nordic Seas when smaller volumes of hosing are applied, allowing for the enhanced deep-convection there to compensate the decreased convection in the Western subpolar gyre. However, a more dedicated experimental set-up and analysis is needed to confirm this hypothesis and fully understand how the spreading of the meltwater may depend on the volume of discharge. In particular, a coupled ice sheet model to capture the main feedback processes between ice sheet, ocean, and atmosphere is desirable.

Meltwater from the Antarctic ice shelf was shown to affect the salt-balance of, in particular, the South Atlantic after 100 years by increasing the Southern Hemisphere super-gyre and the amount of Agulhas leakage entering the South Atlantic (Van den Berk et al. 2019). The AMOC was only marginally affected by this; although the implied changes in north-south density gradient could support AMOC recovery on top of the compensation signal of enhanced deep convection in the Nordic Seas. In this study we were interested to see whether the Southern Hemisphere impact on the AMOC may become stronger on longer timescales. Unfortunately, the present experimental set-up did not allow us to study adjustment processes beyond the year 2195. Haskins et al. (2019), however, did show such impact of slow adjustment in the South Atlantic on AMOC-evolution; in particular it helped AMOC recovery after North Atlantic hosing experiments. It has been suggested in Jüling et al. (2018) that high-resolution models will show faster spreading pathways and adjustment processes; if so, the Antarctic meltwater would also impact the AMOC faster.

The AMOC response to both sources of meltwater thus depends on how the advective processes are represented in a model, and a hierarchy of resolutions would be useful to tease out differences and determine which responses are robust model features. Although the signal of Antarctic freshwater release in the North Atlantic is much smaller than in the South Atlantic, we found clear signs that the

adjustments of the gyres in the subpolar North Atlantic and Nordic Seas were affected by salinity changes originating farther south in the Atlantic.

Acknowledgements This work was funded by the European Commission's 7th Framework Programme, under Grant Agreement number 282672, EMBRACE project. The authors thank the three anonymous referees for their valuable comments and suggestions that have improved the manuscript greatly.

Declarations

Conflicts of interest The authors declare that they have no conflict of interest.

Open Access This article is licensed under a Creative Commons Attribution 4.0 International License, which permits use, sharing, adaptation, distribution and reproduction in any medium or format, as long as you give appropriate credit to the original author(s) and the source, provide a link to the Creative Commons licence, and indicate if changes were made. The images or other third party material in this article are included in the article's Creative Commons licence, unless indicated otherwise in a credit line to the material. If material is not included in the article's Creative Commons licence and your intended use is not permitted by statutory regulation or exceeds the permitted use, you will need to obtain permission directly from the copyright holder. To view a copy of this licence, visit <http://creativecommons.org/licenses/by/4.0/>.

References

- Aagaard K, Carmack EC (1989) The role of sea ice and other fresh water in the Arctic circulation. *J Geophys Res* 94(C10):14,485–14,498. <https://doi.org/10.1029/JC094iC10p14485>
- Bakker P, Schmittner A, Lenaerts J, Abe-Ouchi A, Bi D, van den Broeke M, Chan WL, Hu A, Beadling R, Marsland S et al (2016) Fate of the atlantic meridional overturning circulation: strong decline under continued warming and greenland melting. *Geophys Res Lett* 43(23):12–252
- Bamber JL, Oppenheimer M, Kopp RE, Aspinall WP, Cooke RM (2019) Ice sheet contributions to future sea-level rise from structured expert judgment. *Proc Natl Acad Sci* 116(23):11,195–11,200
- Bindoff NL, Willebrand J, Artale V, Cazenave A, Gregory JM, Gulev S, Hanawa K, Le Quere C, Levitus S, Nojiri Y et al (2007) Observations: oceanic climate change and sea level. In: Solomon S, Qin D, Manning M, Chen Z, Marquis M, Averyt K, Tignor M, Miller H (eds) Climate change 2007: the physical science basis. Cambridge University Press, Cambridge
- Böning CW, Behrens E, Biastoch A, Getzlaff K, Bamber JL (2016) Emerging impact of greenland meltwater on deepwater formation in the north atlantic ocean. *Nat Geosci* 9(7):523–527
- Born A, Mignot J (2012) Dynamics of decadal variability in the Atlantic subpolar gyre: a stochastically forced oscillator. *Clim Dyn* 39(1–2):461–474
- Born A, Stocker TF (2013) Two stable equilibria of the atlantic subpolar gyre. *J Phys Oceanogr* 44(1):246–264. <https://doi.org/10.1175/jpo-d-13-073.1>
- Born A, Stocker TF, Sandø AB (2016) Transport of salt and freshwater in the atlantic subpolar gyre. *Ocean Dyn* 66(9):1051–1064
- Bouillon S, Maqueda MM, Legat V, Fichefet T (2009) An elastic-viscous-plastic sea ice model formulated on Arakawa b and c grid.

- Ocean Modelling 27:174–184. <https://doi.org/10.1016/j.ocemod.2009.01.004>
- Brodeau L, Koenigk T (2016) Extinction of the northern oceanic deep convection in an ensemble of climate model simulations of the 20th and 21st centuries. *Clim Dyn* 46(9–10):2863–2882
- Bulgin CE, Merchant CJ, Ferreira D (2020) Tendencies, variability and persistence of sea surface temperature anomalies. *Sci Rep* 10(1):1–13
- Caesar L, Rahmstorf S, Robinson A, Feulner G, Saba V (2018) Observed fingerprint of a weakening atlantic ocean overturning circulation. *Nature* 556(7700):191–196
- Dansgaard W, Clausen H, Gundestrup N, Hammer C, Johnsen S, Kristinsdottir P, Reeh N (1982) A new greenland deep ice core. *Science* 218(4579):1273–1277
- Deshayes J, Curry R, Msadek R (2014) Cmip5 model intercomparison of freshwater budget and circulation in the north atlantic. *J Clim* 27(9):3298–3317
- Drijfhout S (2015) Competition between global warming and an abrupt collapse of the amoc in earth's energy imbalance. *Sci Rep* 5(14877). <https://doi.org/10.1038/srep14877>
- Drijfhout SS, Weber SL, van der Swaluw E (2011) The stability of the MOC as diagnosed from model projections for pre-industrial, present and future climates. *Clim Dyn* 37(7):1575–1586
- Dukhovskoy D, Yashayaev I, Proshutinsky A, Bamber J, Bashmachnikov I, Chassignet E, Lee C, Tedstone A (2019) Role of greenland freshwater anomaly in the recent freshening of the subpolar north atlantic. *J Geophys Res* 124(5):3333–3360
- ECMWF (2007) IFS documentation. <http://www.ecmwf.int/research/ifsdocs/CY31R1/index.html>
- Feldmann J, Levermann A (2015) Collapse of the west antarctic ice sheet after local destabilization of the amundsen basin. *Proc Natl Acad Sci* 112(46):14,191–14,196
- Fichefet TMMM (1997) Sensitivity of a global sea ice model to the treatment of ice thermodynamics and dynamics. *J Geophys Res* 102(646):609–12. <https://doi.org/10.1029/97JC00480>
- Fu Y, Li F, Karstensen J, Wang C (2020) A stable atlantic meridional overturning circulation in a changing north atlantic ocean since the 1990s. *Sci Adv* 6(48):eabc7836
- Fyke J, Sergienko O, Löfverström M, Price S, Lenaerts JT (2018) An overview of interactions and feedbacks between ice sheets and the earth system. *Rev Geophys* 56(2):361–408
- Gary SF, Lozier MS, Böning CW, Biastoch A (2011) Deciphering the pathways for the deep limb of the meridional overturning circulation. *Deep Sea Res Part II* 58(17):1781–1797
- Garzoli SL, Baringer MO, Dong S, Perez RC, Yao Q (2013) South Atlantic meridional fluxes. *Deep Sea Res Part I Oceanogr Res Papers* 71:21–32
- Gillard LC, Hu X, Myers PG, Bamber JL (2016) Meltwater pathways from marine terminating glaciers of the greenland ice sheet. *Geophys Res Lett.* <https://doi.org/10.1002/2016GL070969>
- Haskins RK, Oliver KI, Jackson LC, Drijfhout SS, Wood RA (2019) Explaining asymmetry between weakening and recovery of the amoc in a coupled climate model. *Clim Dyn* 53(1–2):67–79
- Haskins RK, Oliver KI, Jackson LC, Wood RA, Drijfhout SS (2020) Temperature domination of amoc weakening due to freshwater hosing in two gcms. *Clim Dyn* 54(1–2):273–286
- Hazeleger W, Wang X, Severijns C, Štefanescu S, Bintanja R, Sterl A, Wyser K, Semmler T, Yang S, Hurk B, Noije T, Linden E, Wiel K (2012) Ec-earth v2.2: description and validation of a new seamless earth system prediction model. *Clim Dyn* 39(11):2611–2629. <https://doi.org/10.1007/s00382-011-1228-5>
- Helm V, Humbert A, Miller H (2014) Elevation and elevation change of greenland and antarctica derived from cryosat-2. *The Cryosphere* 8(4):1539–1559
- Hurrell JW (1995) Decadal trends in the north atlantic oscillation: regional temperatures and precipitation. *Science* 269(5224):676–679
- Hurrell JW, Kushnir Y, Ottersen G, Visbeck M (2003) An overview of the north atlantic oscillation. *Geophys Monograph-Am Geophys Union* 134:1–36
- Jackson LC, Schaller N, Smith RS, Palmer MD, Vellinga M (2013) Response of the Atlantic meridional overturning circulation to a reversal of greenhouse gas increases. *Clim Dyn.* <https://doi.org/10.1007/s00382-013-1842-5>
- Johnsen S, Clausen HB, Dansgaard W, Fuhrer K, Gundestrup N, Hammer CU, Iversen P, Jouzel J, Stauffer B et al (1992) Irregular glacial interstadials recorded in a new greenland ice core. *Nature* 359(6393):311–313
- Joughin I, Smith BE, Medley B (2014) Marine ice sheet collapse potentially under way for the thwaites glacier basin, west antarctica. *Science* 344(6185):735–738
- Jüling A, Viebahn JP, Drijfhout SS, Dijkstra HA (2018) Energetics of the southern ocean mode. *J Geophys Res* 123(12):9283–9304
- Karstensen J, Lorbacher K (2011) A practical indicator for surface ocean heat and freshwater buoyancy fluxes and its application to the ncep reanalysis data. *Tellus A* 63(2). <https://doi.org/10.1111/j.1600-0870.2011.00510.x>
- Lavender KL, Davis RE, Owens WB (2000) Mid-depth recirculation observed in the interior labrador and irminger seas by direct velocity measurements. *Nature* 407(6800):66–69
- Le Corre M, Gula J, Tréguier AM (2020) Barotropic vorticity balance of the north atlantic subpolar gyre in an eddy-resolving model. *Ocean Sci* 16(2):451–468. <https://doi.org/10.5194/os-16-451-2020>, <https://os.copernicus.org/articles/16/451/2020/>
- Lohmann K, Jungclaus JH, Matei D, Mignot J, Menary M, Langehaug H, Ba J, Gao Y, Otterå O, Park W et al (2014) The role of subpolar deep water formation and nordic seas overflows in simulated multidecadal variability of the atlantic meridional overturning circulation. *Ocean Sci* 10:227–241
- Lozier M, Li F, Bacon S, Bahr F, Bower A, Cunningham S, De Jong M, De Steur L, Deyoung B, Fischer J et al (2019) A sea change in our view of overturning in the subpolar north atlantic. *Science* 363(6426):516–521
- Luyten J, Stommel H (1986) Gyres driven by combined wind and buoyancy flux. *J Phys Oceanography* 16(9):1551–1560. [https://doi.org/10.1175/1520-0485\(1986\)016151:GDBCA2.0.CO;2](https://doi.org/10.1175/1520-0485(1986)016151:GDBCA2.0.CO;2)
- Madec G (2008) NEMO ocean engine. Note du Pole de modelisation, Institut Pierre-Simon Laplace (IPSL). France 27:1288–1619
- Manabe S, Stouffer R (1988) Two stable equilibria of a coupled ocean-atmosphere model. *J Clim* 1(9):841–866
- Marotzke J (1997) Boundary mixing and the dynamics of three-dimensional thermohaline circulations. *J Phys Oceanography* 27(8):1713–1728
- McDougall TJ, Feistel R, Millero FJ, Jackett DR, Wright DG, King BA, Pawlowicz R, Marion GM, Chen CTA, Spitzer P, Seitz S (2009) The international thermodynamic equation of seawater 2010 (teos-10): calculation and use of thermodynamic properties. Global ship-based repeat hydrography manual, IOCCP report no, 14
- Mecking J, Drijfhout S, Jackson L, Andrews M (2017) The effect of model bias on atlantic freshwater transport and implications for amoc bi-stability. *Tellus A Dyn Meteorol Oceanogr* 69(1):1299, 910. <https://doi.org/10.1080/16000870.2017.1299910>
- Moat BI, Smeed DA, Frajka-Williams E, Desbruyères DG, Beaulieu C, Johns WE, Rayner D, Sanchez-Franks A, Baringer MO, Volkov D, Jackson LC, Bryden HL (2020) Pending recovery in the strength of the meridional overturning circulation at 26 n. *Ocean Sci* 16(4):863–874. <https://doi.org/10.5194/os-16-863-2020>, <https://os.copernicus.org/articles/16/863/2020/>

- Mouginot J, Rignot E, Bjørk AA, Van Den Broeke M, Millan R, Morlighem M, Noël B, Scheuchl B, Wood M (2019) Forty-six years of greenland ice sheet mass balance from 1972 to 2018. *Proc Natl Acad Sci* 116(19):9239–9244
- Paolo FS, Fricker HA, Padman L (2015) Volume loss from antarctic ice shelves is accelerating. *Science* 348(6232):327–331
- Pedlosky J (1996) Ocean Circulation Theory. Springer Science & Business Media, Berlin
- Pörtner H, Roberts D, Masson-Delmotte V, Zhai P, Tignor M, Poloczanska E, Mintenbeck K, Alegria A, Nicolai M, Okem A, Petzold J, Rama B, Weyer NM (eds) (2019) IPCC 2019: IPCC special report on the ocean and cryosphere in a changing climate. (In press)
- Rahmstorf S (1996) On the freshwater forcing and transport of the Atlantic thermohaline circulation. *Clim Dyn* 12(12):799–811
- Rhein M, Steinfeldt R, Kieke D, Stendardo I, Yashayaev I (2017) Ventilation variability of labrador sea water and its impact on oxygen and anthropogenic carbon: a review. *Philos Trans R Soc A* 375(2102):20160321. <https://doi.org/10.1098/rsta.2016.0321>
- Rignot E, Mouginot J, Morlighem M, Seroussi H, Scheuchl B (2014) Widespread, rapid grounding line retreat of pine island, thwaites, smith, and kohler glaciers, west antarctica, from 1992 to 2011. *Geophys Res Lett* 41(10):3502–3509
- Sgubin G, Swingedouw D, Drijfhout S, Hagemann S, Robertson E (2014) Multimodel analysis on the response of the AMOC under an increase of radiative forcing and its symmetrical reversal. *Clim Dyn.* <https://doi.org/10.1007/s00382-014-2391-2>
- Sgubin G, Swingedouw D, Drijfhout S, Mary Y, Bennabi A (2017) Abrupt cooling over the north atlantic in modern climate models. *Nat Commun.* <https://doi.org/10.1038/ncomms14375>
- Shepherd A, Gilbert L, Muir AS, Konrad H, McMillan M, Slater T, Briggs KH, Sundal AV, Hogg AE, Engdahl ME (2019) Trends in antarctic ice sheet elevation and mass. *Geophys Res Lett* 46(14):8174–8183
- Sijp WP, Gregory JM, Tailleux R, Spence P (2012) The key role of the western boundary in linking the amoc strength to the north-south pressure gradient. *J Phys Oceanography* 42(4):628–643
- Smeed DA, Josey S, Beaulieu C, Johns WE, Moat BI, Frajka-Williams E, Rayner D, Meinen CS, Baringer MO, Bryden HL et al (2018) The north atlantic ocean is in a state of reduced overturning. *Geophys Res Lett* 45(3):1527–1533
- Spall MA, Pickart RS (2001) Where does dense water sink? a subpolar gyre example. *J Phys Oceanography* 31(3):810–826. [https://doi.org/10.1175/1520-0485\(2001\)0310810:WDDWSA2.0.CO;2](https://doi.org/10.1175/1520-0485(2001)0310810:WDDWSA2.0.CO;2)
- Starr A, Hall IR, Barker S, Rackow T, Zhang X, Hemming SR, van der Lubbe HJL, Knorr G, Berke MA, Bigg GR, Cartagena-Sierra A, Jiménez-Espejo FJ, Gong X, Gruetzsner J, Lathika N, LeVay LJ, Robinson RS, Ziegler M, Brentegani L, Caley T, Charles CD, Coenen JJ, Crespin JG, Franzese AM, Han X, Hines SKV, Jimenez Espejo FJ, Just J, Koutsodendris A, Kubota K, Norris RD, dos Santos TP, Rolison JM, Simon MH, Tangunan D, van der Lubbe HJL, Yamane M, Zhang H, Party ES (2021) Antarctic icebergs reorganize ocean circulation during pleistocene glacials. *Nature* 589(1):236–241. <https://doi.org/10.1038/s41586-020-03094-7>
- Sterl A, Bintanja R, Brodeau L, Gleeson E, Koenigk T, Schmitt T, Semmler T, Severijns C, Wyser K, Yang S (2012) A look at the ocean in the ec-earth climate model. *Clim Dyn* 39(11):2631–2657
- Stouffer RJ, Yin J, Gregory J, Dixon K, Spelman M, Hurlin W, Weaver A, Eby M, Flato G, Hasumi H et al (2006) Investigating the causes of the response of the thermohaline circulation to past and future climate changes. *J Clim* 19(8):1365–1387
- Swingedouw D, Fichefet T, Goosse H, Loutre MF (2009) Impact of transient freshwater releases in the southern ocean on the amoc and climate. *Clim Dyn* 33(2–3):365–381
- Swingedouw D, Rodehacke CB, Behrens E, Menary M, Olsen SM, Gao Y, Mikolajewicz U, Mignot J, Biastoch A (2013) Decadal fingerprints of freshwater discharge around greenland in a multi-model ensemble. *Clim Dyn* 41(3–4):695–720
- Swingedouw D, Rodehacke CB, Olsen SM, Menary M, Gao Y, Mikolajewicz U, Mignot J (2015) On the reduced sensitivity of the atlantic overturning to greenland ice sheet melting in projections: a multi-model assessment. *Clim Dyna* 44(11–12):3261–3279
- Taylor KE, Stouffer RJ, Meehl GA (2012) An overview of CMIP5 and the experiment design. *Bull Am Meteorol Soc* 93(4):485–498. <https://doi.org/10.1175/BAMS-D-11-00094.1>
- Thorpe RB, Gregory JM, Johns TC, Wood RA, Mitchell JFB (2001) Mechanisms determining the atlantic thermohaline circulation response to greenhouse gas forcing in a non-flux-adjusted coupled climate model. *J Clim* 14(14):3102–3116. [https://doi.org/10.1175/1520-0442\(2001\)0143102:MDTATC2.0.CO;2](https://doi.org/10.1175/1520-0442(2001)0143102:MDTATC2.0.CO;2)
- Valcke S, Caubel A, Vogelsang R, Declat D (2004) OASIS 3 user's guide. Technical report TR/CMGC/04/68, CERFACS
- Van den Berk J, Drijfhout S (2014) A realistic freshwater forcing protocol for ocean-coupled climate models. *Ocean Modelling* 81:36–48. <https://doi.org/10.1016/j.ocemod.2014.07.003>
- Van den Berk J, Drijfhout S, Hazeleger W (2019) Atlantic salinity budget in response to northern and southern hemisphere ice sheet discharge. *Clim Dyn* 52(9–10):5249–5267
- Vellinga M, Wood RA (2002) Global climatic impacts of a collapse of the atlantic thermohaline circulation. *Clim Change* 54(3):251–267
- Colin de Verdière A (1989) On the interaction of wind and buoyancy driven gyres. *J Marine Res* 47(3):595–633. <https://doi.org/10.1357/002224089785076172>
- Wary M, Eynaud F, Swingedouw D, Masson-Delmotte V, Matthiessen J, Kissel C, Zumaque J, Rossignol L, Jouzel J (2017) Regional seesaw between the north atlantic and nordic seas during the last glacial abrupt climate events. *Clim Past* 13(6):729–739
- Weber S, Drijfhout S, Abe-Ouchi A, Crucifix M, Eby M, Ganopolski A, Murakami S, Otto-Btiesner B, Peltier W (2007) The modern and glacial overturning circulation in the atlantic ocean in pmip coupled model simulations. *Clim Past* 3:51–64
- Weijer W, De Ruijter WP, Sterl A, Drijfhout SS (2002) Response of the atlantic overturning circulation to south atlantic sources of buoyancy. *Global Planetary Change* 34(3–4):293–311
- Weijer W, Maltrud ME, Hecht MW, Dijkstra HA, Kliphus MA (2012) Response of the Atlantic ocean circulation to Greenland ice sheet melting in a strongly-eddy ocean model. *Geophys Res Lett.* <https://doi.org/10.1029/2012GL051611>
- Wood RA, Keen AB, Mitchell JF, Gregory JM (1999) Changing spatial structure of the thermohaline circulation in response to atmospheric CO₂ forcing in a climate model. *Nature* 399(6736):572–575
- Wouters B, Drijfhout S, Hazeleger W (2012) Interdecadal north-atlantic meridional overturning circulation variability in ec-earth. *Clim Dyn* 39(11):2695–2712
- Yang Q, Dixon TH, Myers PG, Bonin J, Chambers D, Van Den Broeke M (2016) Recent increases in arctic freshwater flux affects labrador sea convection and atlantic overturning circulation. *Nat Commun* 7(1):1–8. <https://doi.org/10.1038/ncomms10525>
- Zhang R, Delworth TL, Rosati A, Anderson WG, Dixon KW, Lee HC, Zeng F (2011) Sensitivity of the north atlantic ocean circulation to an abrupt change in the nordic sea overflow in a high resolution global coupled climate model. *J Geophys Res Oceans* 116(C12):c12024. <https://doi.org/10.1029/2011JC007240>

Publisher's Note Springer Nature remains neutral with regard to jurisdictional claims in published maps and institutional affiliations.